Fermi-Dirac Correlations in Λ Pairs in Hadronic Z Decays

R. Barate, D. Decamp, P. Ghez, C. Goy, J.P. Lees, F. Martin, E. Merle, M.N. Minard, B. Pietrzyk, R. Alemany, et al.

EUROPEAN LABORATORY FOR PARTICLE PHYSICS (CERN)

CERN EP/99-172
8 December, 1999

Fermi-Dirac Correlations in Λ Pairs in Hadronic Z Decays

The ALEPH Collaboration*)

Abstract

Two-particle correlations of $\Lambda\Lambda$ and $\bar{\Lambda}\bar{\Lambda}$ pairs have been studied in multihadronic Z decays recorded with the ALEPH detector at LEP in the years from 1992 to 1995. The correlations were measured as a function of the four-momentum difference Q of the pair. A depletion of events is observed in the region $Q < 2$ GeV which could arise from the effects of Fermi-Dirac statistics. In addition the spin content of the Λ pair system has been determined. For $Q > 2$ GeV the fraction of pairs with spin one is consistent with the value of 0.75 expected for a statistical spin mixture, whilst for $Q < 2$ GeV this fraction is found to be lower. For $\Lambda\bar{\Lambda}$ pairs, where no Fermi-Dirac correlations are expected, the spin one fraction is measured to be consistent with 0.75 over the entire analysed Q range.

(Submitted to Physics Letters B)

*) See next pages for the list of authors

The ALEPH Collaboration

R. Barate, D. Decamp, P. Ghez, C. Goy, J.-P. Lees, F. Martin, E. Merle, M.-N. Minard, B. Pietrzyk

Laboratoire de Physique des Particules (LAPP), IN^{2}P^3-CNRS, F-74019 Annecy-le-Vieux Cedex, France

R. Alemany, S. Bravo, M.P. Casado, M. Chmeissani, J.M. Crespo, E. Fernandez, M. Fernandez-Bosman, Ll. Garrido,[15] E. Graugès, A. Juste, M. Martinez, G. Merino, R. Miquel, Ll.M. Mir, A. Pacheco, I. Riu, H. Ruiz

Institut de Física d'Altes Energies, Universitat Autònoma de Barcelona, E-08193 Bellaterra (Barcelona), Spain[7]

A. Colaleo, D. Creanza, M. de Palma, G. Iaselli, G. Maggi, M. Maggi, S. Nuzzo, A. Ranieri, G. Raso, F. Ruggieri, G. Selvaggi, L. Silvestris, P. Tempesta, A. Tricomi,[3] G. Zito

Dipartimento di Fisica, INFN Sezione di Bari, I-70126 Bari, Italy

X. Huang, J. Lin, Q. Ouyang, T. Wang, Y. Xie, R. Xu, S. Xue, J. Zhang, L. Zhang, W. Zhao

Institute of High-Energy Physics, Academia Sinica, Beijing, The People's Republic of China[8]

D. Abbaneo, G. Boix,[6] O. Buchmüller, M. Cattaneo, F. Cerutti, V. Ciulli, G. Dissertori, H. Drevermann, R.W. Forty, M. Frank, T.C. Greening, A.W. Halley, J.B. Hansen, J. Harvey, P. Janot, B. Jost, I. Lehraus, O. Leroy, P. Mato, A. Minten, A. Moutoussi, F. Ranjard, L. Rolandi, D. Schlatter, M. Schmitt,[20] O. Schneider,[2] P. Spagnolo, W. Tejessy, F. Teubert, E. Tournefier, A.E. Wright

European Laboratory for Particle Physics (CERN), CH-1211 Geneva 23, Switzerland

Z. Ajaltouni, F. Badaud, G. Chazelle, O. Deschamps, A. Falvard, C. Ferdi, P. Gay, C. Guicheney, P. Henrard, J. Jousset, B. Michel, S. Monteil, J-C. Montret, D. Pallin, P. Perret, F. Podlyski

Laboratoire de Physique Corpusculaire, Université Blaise Pascal, IN^{2}P^3-CNRS, Clermont-Ferrand, F-63177 Aubière, France

J.D. Hansen, J.R. Hansen, P.H. Hansen, B.S. Nilsson, B. Rensch, A. Wäänänen

Niels Bohr Institute, DK-2100 Copenhagen, Denmark[9]

G. Daskalakis, A. Kyriakis, C. Markou, E. Simopoulou, I. Siotis, A. Vayaki

Nuclear Research Center Demokritos (NRCD), GR-15310 Attiki, Greece

A. Blondel, G. Bonneaud, J.-C. Brient, A. Rougé, M. Rumpf, M. Swynghedauw, M. Verderi, H. Videau

Laboratoire de Physique Nucléaire et des Hautes Energies, Ecole Polytechnique, IN^{2}P^3-CNRS, F-91128 Palaiseau Cedex, France

E. Focardi, G. Parrini, K. Zachariadou

Dipartimento di Fisica, Università di Firenze, INFN Sezione di Firenze, I-50125 Firenze, Italy

M. Corden, C. Georgiopoulos

Supercomputer Computations Research Institute, Florida State University, Tallahassee, FL 32306-4052, USA [13,14]

A. Antonelli, G. Bencivenni, G. Bologna,[4] F. Bossi, P. Campana, G. Capon, V. Chiarella, P. Laurelli, G. Mannocchi,[1,5] F. Murtas, G.P. Murtas, L. Passalacqua, M. Pepe-Altarelli

Laboratori Nazionali dell'INFN (LNF-INFN), I-00044 Frascati, Italy

L. Curtis, J.G. Lynch, P. Negus, V. O'Shea, C. Raine, P. Teixeira-Dias, A.S. Thompson

Department of Physics and Astronomy, University of Glasgow, Glasgow G12 8QQ,United Kingdom[10]

R. Cavanaugh, S. Dhamotharan, C. Geweniger,[1] P. Hanke, G. Hansper, V. Hepp, E.E. Kluge, A. Putzer, J. Sommer, K. Tittel, S. Werner,[19] M. Wunsch[19]

Institut für Hochenergiephysik, Universität Heidelberg, D-69120 Heidelberg, Germany[16]

R. Beuselinck, D.M. Binnie, W. Cameron, P.J. Dornan,[1] M. Girone, S. Goodsir, E.B. Martin, N. Marinelli, A. Sciabà, J.K. Sedgbeer, E. Thomson, M.D. Williams

Department of Physics, Imperial College, London SW7 2BZ, United Kingdom[10]

V.M. Ghete, P. Girtler, E. Kneringer, D. Kuhn, G. Rudolph

Institut für Experimentalphysik, Universität Innsbruck, A-6020 Innsbruck, Austria[18]

C.K. Bowdery, P.G. Buck, A.J. Finch, F. Foster, G. Hughes, R.W.L. Jones, N.A. Robertson, M.I. Williams

Department of Physics, University of Lancaster, Lancaster LA1 4YB, United Kingdom[10]

I. Giehl, K. Jakobs, K. Kleinknecht, G. Quast, B. Renk, E. Rohne, H.-G. Sander, H. Wachsmuth, C. Zeitnitz

Institut für Physik, Universität Mainz, D-55099 Mainz, Germany[16]

J.J. Aubert, A. Bonissent, J. Carr, P. Coyle, P. Payre, D. Rousseau

Centre de Physique des Particules, Faculté des Sciences de Luminy, IN^{2}P^3-CNRS, F-13288 Marseille, France

M. Aleppo, M. Antonelli, F. Ragusa

Dipartimento di Fisica, Università di Milano e INFN Sezione di Milano, I-20133 Milano, Italy

V. Büscher, H. Dietl, G. Ganis, K. Hüttmann, G. Lütjens, C. Mannert, W. Männer, H.-G. Moser, S. Schael, R. Settles, H. Seywerd, H. Stenzel, W. Wiedenmann, G. Wolf

Max-Planck-Institut für Physik, Werner-Heisenberg-Institut, D-80805 München, Germany[16]

P. Azzurri, J. Boucrot, O. Callot, S. Chen, A. Cordier, M. Davier, L. Duflot, J.-F. Grivaz, Ph. Heusse, A. Jacholkowska,[1] F. Le Diberder, J. Lefrançois, A.-M. Lutz, M.-H. Schune, J.-J. Veillet, I. Videau,[1] D. Zerwas

Laboratoire de l'Accélérateur Linéaire, Université de Paris-Sud, IN^{2}P^3-CNRS, F-91898 Orsay Cedex, France

G. Bagliesi, T. Boccali, C. Bozzi,[12] G. Calderini, R. Dell'Orso, I. Ferrante, L. Foà, A. Giassi, A. Gregorio, F. Ligabue, P.S. Marrocchesi, A. Messineo, F. Palla, G. Rizzo, G. Sanguinetti, G. Sguazzoni, R. Tenchini, A. Venturi, P.G. Verdini

Dipartimento di Fisica dell'Università, INFN Sezione di Pisa, e Scuola Normale Superiore, I-56010 Pisa, Italy

G.A. Blair, G. Cowan, M.G. Green, T. Medcalf, J.A. Strong

Department of Physics, Royal Holloway & Bedford New College, University of London, Surrey TW20 OEX, United Kingdom[10]

D.R. Botterill, R.W. Clifft, T.R. Edgecock, P.R. Norton, J.C. Thompson, I.R. Tomalin

Particle Physics Dept., Rutherford Appleton Laboratory, Chilton, Didcot, Oxon OX11 OQX, United Kingdom[10]

B. Bloch-Devaux, P. Colas, S. Emery, W. Kozanecki, E. Lançon, M.-C. Lemaire, E. Locci, P. Perez, J. Rander, J.-F. Renardy, A. Roussarie, J.-P. Schuller, J. Schwindling, A. Trabelsi,[21] B. Vallage

CEA, DAPNIA/Service de Physique des Particules, CE-Saclay, F-91191 Gif-sur-Yvette Cedex, France[17]

S.N. Black, J.H. Dann, R.P. Johnson, H.Y. Kim, N. Konstantinidis, A.M. Litke, M.A. McNeil, G. Taylor

Institute for Particle Physics, University of California at Santa Cruz, Santa Cruz, CA 95064, USA[22]

C.N. Booth, S. Cartwright, F. Combley, M. Lehto, L.F. Thompson

Department of Physics, University of Sheffield, Sheffield S3 7RH, United Kingdom[10]

K. Affholderbach, A. Böhrer, S. Brandt, C. Grupen, J. Hess, A. Misiejuk, G. Prange, U. Sieler

Fachbereich Physik, Universität Siegen, D-57068 Siegen, Germany[16]

G. Giannini, B. Gobbo

Dipartimento di Fisica, Università di Trieste e INFN Sezione di Trieste, I-34127 Trieste, Italy

J. Rothberg, S. Wasserbaech

Experimental Elementary Particle Physics, University of Washington, WA 98195 Seattle, U.S.A.

S.R. Armstrong, P. Elmer, D.P.S. Ferguson, Y. Gao, S. González, O.J. Hayes, H. Hu, S. Jin, J. Kile, P.A. McNamara III, J. Nielsen, W. Orejudos, Y.B. Pan, Y. Saadi, I.J. Scott, J. Walsh, J.H. von Wimmersperg-Toeller, Sau Lan Wu, X. Wu, G. Zobernig

Department of Physics, University of Wisconsin, Madison, WI 53706, USA[11]

[1]Also at CERN, 1211 Geneva 23, Switzerland.

[2]Now at Université de Lausanne, 1015 Lausanne, Switzerland.

[3]Also at Centro Siciliano di Fisica Nucleare e Struttura della Materia, INFN, Sezione di Catania, 95129 Catania, Italy.

[4]Also Istituto di Fisica Generale, Università di Torino, 10125 Torino, Italy.

[5]Also Istituto di Cosmo-Geofisica del C.N.R., Torino, Italy.

[6]Supported by the Commission of the European Communities, contract ERBFMBICT982894.

[7]Supported by CICYT, Spain.

[8]Supported by the National Science Foundation of China.

[9]Supported by the Danish Natural Science Research Council.

[10]Supported by the UK Particle Physics and Astronomy Research Council.

[11]Supported by the US Department of Energy, grant DE-FG0295-ER40896.

[12]Now at INFN Sezione de Ferrara, 44100 Ferrara, Italy.

[13]Supported by the US Department of Energy, contract DE-FG05-92ER40742.

[14]Supported by the US Department of Energy, contract DE-FC05-85ER250000.

[15]Permanent address: Universitat de Barcelona, 08208 Barcelona, Spain.

[16]Supported by the Bundesministerium für Bildung, Wissenschaft, Forschung und Technologie, Germany.

[17]Supported by the Direction des Sciences de la Matière, C.E.A.

[18]Supported by Fonds zur Förderung der wissenschaftlichen Forschung, Austria.

[19]Now at SAP AG, 69185 Walldorf, Germany.

[20]Now at Harvard University, Cambridge, MA 02138, U.S.A.

[21]Now at Département de Physique, Faculté des Sciences de Tunis, 1060 Le Belvédère, Tunisia.

[22]Supported by the US Department of Energy, grant DE-FG03-92ER40689.

1 Introduction

Studies of Bose-Einstein (BE) correlations of identical bosons and of Fermi-Dirac (FD) correlations of identical fermions produced in high energy collisions provide measurements of the distribution of the particle sources in space and time. These correlations originate from the symmetrization or antisymmetrization of the two-particle wave functions of identical particles and lead to an enhancement or a suppression of particle pairs produced close to each other in phase space. This effect is sensitive to the size of the source from which the identical particles of similar momenta are emitted. A description of the theory can be found e.g., in references [1], [2] and [3].

This paper reports on a study of Fermi-Dirac correlations using the combined sample of $\Lambda\Lambda$ and $\bar{\Lambda}\bar{\Lambda}$ pairs (represented by $(\Lambda\Lambda)$ throughout this paper) reconstructed by ALEPH in multihadronic Z decays at LEP 1. Section 2 summarizes the theory of Fermi-Dirac correlations and the techniques used to study these correlations. Section 3 describes the ALEPH detector and the selection of neutral Λ decays. The results are presented in Section 4 and are followed by the conclusions in Section 5.

2 Theory

The strength of two-particle BE or FD correlation effects can be expressed in terms of a two-particle correlation function $C(p_1, p_2)$ defined as

$$C(p_1, p_2) = P(p_1, p_2)/P_0(p_1, p_2) \; , \tag{1}$$

where p_1 and p_2 are the four-momenta of the particles, $P(p_1, p_2)$ is the measured differential cross section for the pairs and $P_0(p_1, p_2)$ is that of a reference sample, which is free of BE or FD correlations but otherwise identical in all aspects to the data sample. The main experimental difficulty is to define an appropriate reference sample $P_0(p_1, p_2)$ in order to determine that part of $P(p_1, p_2)$ which can be attributed to the BE or FD correlations. An example for such a reference sample is given by the JETSET Monte Carlo [4] for which production of hadrons is simulated without taking into account BE or FD correlation effects.

The correlation function C is usually measured as a function of the Lorentz invariant Q with $Q^2 = -(p_1 - p_2)^2$. For $Q^2 = 0$ the effects of BE and FD correlations reach their extreme values. Various parametrisations for $C(Q)$ are proposed in the literature. Here the GGLP parametrisation [5]

$$C(Q) = \mathcal{N}[1 + \beta \exp(-R^2 Q^2)] \tag{2a}$$

is used, together with an alternative parametrisation [6]

$$C(Q) = \mathcal{N}[1 + \beta \exp(-RQ)] \tag{2b}$$

for comparison. The form of Eq. 2a is expected for a spherical source with a Gaussian density distribution in the rest frame of the emitted pair. The free parameters are the normalisation $\mathcal{N}$, the suppression parameter β ($|\beta| \leq 1$) and the radius R, which can be identified with the space-time extent of the source. In two-boson systems a value of $\beta = 1$ corresponds to a completely incoherent emission; $|\beta|$ is expected to be different from unity if sources of different radii (for example, due to different resonance lifetimes) contribute to the emission of the pairs [7] or if the particles have non-zero spin as explained below. This parameter also accomodates for experimental backgrounds such as particle misidentification.

The total wave function describing the final state of two identical particles must be either symmetric (s) or antisymmetric (a) under the exchange of the two particles, depending on the spin statistics of the particles. In the limit of plane waves (i.e., neglecting contributions from possible final state interactions) this leads to [8]

$$|\Psi_{s,a}|^2 = 1 \pm \cos[(p_1 - p_2) \cdot (r_1 - r_2)] \,, \tag{3}$$

where s (a) corresponds to the $+$ ($-$) sign and $r_{1,2}$ are the four-vector positions of the two particles. In the case of identical spinless bosons, Ψ_s completely describes the final state, whereas in the case of identical fermions both Ψ_s and Ψ_a can contribute.

Since $P_{s,a}(p_1, p_2)$ is proportional to the integral $\int dr_1 dr_2 g(r_1, r_2, p_1, p_2)|\Psi_{s,a}|^2$, where $g(r_1, r_2, p_1, p_2)$ describes the source intensity and the integral is taken over the relative space-time distances $r_1 - r_2$ of the particle emission points, it follows that the correlation function $C_{s,a}(p_1, p_2)$ for the symmetric (antisymmetric) final state should show an increase (decrease) for $Q \to 0$.

For identical bosons with spin or identical fermions, e.g., two Λ's, one has also to consider their spin. For the ($\Lambda\Lambda$) system the total spin may be $S = 0$ or $S = 1$ with spin wave functions s_0 and s_1^i, where $i = -1, 0, 1$ are the eigenvalues of the third component of the total spin; s_0 is antisymmetric whereas the s_1^i are symmetric under the exchange of the two Λ's. As the total wave function for the ($\Lambda\Lambda$) system is antisymmetric, s_0 must be combined with Ψ_s from Eq. 3 and the s_1^i with Ψ_a to yield antisymmetric wave functions: $\Theta_0 = \Psi_s s_0$ and $\Theta_1^i = \Psi_a s_1^i$. In general both Θ_0 and the Θ_1^i can contribute to $P(p_1, p_2)$, depending on the source. However for a statistical spin mixture ensemble, where each of the four spin states s_0 and s_1^i is emitted with the same probability, the contributions from the Θ_1^i will dominate by a factor of 3 and thus the correlation function $C(Q)$ is expected to decrease to 0.5 as Q tends to zero.

A different way of investigating the ($\Lambda\Lambda$) correlations is provided by the measurement of the spin composition of the ($\Lambda\Lambda$) system, that is to determine the fractions of the $S = 0$ and $S = 1$ states. The method used in this paper was proposed in Ref. [9] and is based on the measurement of the distribution dN/dy^* in the di-hyperon centre-of-mass system. In this system the momenta of the decay protons (antiprotons) of the ($\Lambda\Lambda$) system are transformed into their parent hyperon rest frames and y^* is then the cosine of the angle between the two protons (antiprotons). From the Wigner-Eckart theorem [10] the angular distributions for the $S = 0$ and $S = 1$ states of a system of identical hyperons are

$$dN/dy^*|_{S=0} \quad = \quad (N/2)(1 - \alpha_\Lambda^2 y^*) \tag{4a}$$

and

$$dN/dy^*|_{S=1} \quad = \quad (N/2)(1 + (\alpha_\Lambda^2/3)y^*) \tag{4b}$$

where $\alpha_\Lambda = -\alpha_{\bar{\Lambda}} = 0.642 \pm 0.013$ is the Λ decay asymmetry parameter [11]. In general both spin states will contribute. If the parameter ε is defined as the fraction of the $S = 1$ contribution, then ε can be measured as a function of Q by fitting the expression

$$dN/dy^* = (1 - \varepsilon)dN/dy^*|_{S=0} + \varepsilon dN/dy^*|_{S=1} \tag{4c}$$

to the measured distribution for a given range of Q. In the case of a statistical spin mixture, ε is equal to 0.75 which results in a constant distribution for dN/dy^*. The advantage of this method is that a reference sample is not needed. In Ref. [9] the relation in Eq. 4 was derived for the di-hyperon threshold and also shown to hold approximately for low values of Q, where the relative momentum of the two Λ's is non-relativistic. It was recently pointed out, however, that the validity range for Eq. 4 can be extended to any Q value [12].

The correlation function $C(Q)$ and the spin composition $\varepsilon(Q)$ yield different measurements which are sensitive to the same physical effect. If a source only emitted di-hyperons in a total spin state $S = 1$ or $S = 0$, then $\varepsilon(Q)$ would be one or zero, respectively, independent of Q, whereas the correlation function $C(Q)$ is still expected to show a Q dependence.

The quantity $\varepsilon(Q)$ can also be used to estimate the size R of the source [12]. If $C(Q)_{S=0}$ and $C(Q)_{S=1}$ are respectively the contributions of the $S = 0$ and the $S = 1$ states to $C(Q)$, then for a statistical spin mixture ensemble $C(Q)_{S=0}$ and $C(Q)_{S=1}$ can be parametrised with the formula of Eq. 2a as

$$C(Q)_{S=0} \quad = \quad 0.25\mathcal{N}(1 + \gamma \exp(-R^2Q^2))$$

and

$$C(Q)_{S=1} \quad = \quad 0.75\mathcal{N}(1 - \gamma \exp(-R^2Q^2))$$

with $|\gamma| \leq 1$. With $\varepsilon(Q) = C(Q)_{S=1}/(C(Q)_{S=0} + C(Q)_{S=1})$ one finds

$$\varepsilon(Q) = 0.75(1 - \gamma \exp(-R^2Q^2))/(1 - 0.5\gamma \exp(-R^2Q^2)) \ , \tag{5}$$

where the suppression parameter $\gamma = -2\beta$ results from the requirement $C(Q)_{S=0} + C(Q)_{S=1} = C(Q)$, with $C(Q)$ defined in Eq. 2a. In the ideal case $C(Q)_{S=1}$ is expected to decrease to zero as Q tends to zero which implies $\gamma = 1$. But due to the effects described before in connection with Eq. 2, γ can deviate from one.

3 The ALEPH Detector and Data Selection

The ALEPH detector is described in detail elsewhere [13]. This analysis relies mainly on the information from three concentric tracking detectors, a 1.8 m radius time projection chamber (TPC) surrounding a small conventional drift chamber (ITC) and a two layer silicon vertex detector (VDET). The TPC provides up to 21 space points per track and in addition up to 338 samples of the particle's specific ionisation. The ITC measures 8 points per track and the VDET provides two high precision space points on the track near the primary vertex. The tracking detectors are located in an axial magnetic field of 1.5 T and have a combined track transverse momentum resolution of $\Delta p_\perp / p_\perp = 0.0006 p_\perp \oplus 0.005$ (with $p_\perp$ in GeV/c).

The analysis was performed on data collected on and around the Z peak. The event sample consists of a total of 3.9 million hadronic events corresponding to an integrated luminosity of 142 pb^{-1}. A sample of 6.5 million Monte Carlo events with full detector simulation [13], based on the JETSET 7.4 [4] generator, was used to provide a reference sample and to calculate the selection efficiencies as described in Section 4. This Monte Carlo sample does not include BE or FD correlations.

Hadronic events were required to contain at least five well reconstructed tracks. Each such track must have at least four TPC hits and a polar angle in the range $|\cos\theta| < 0.95$. The point of closest approach of the reconstructed tracks to the beam axis must be within 10 cm of the nominal interaction point along the beam direction and within 2 cm of it in the plane transverse to the beam. The total energy of all tracks satisfying the above cuts is required to be at least 10% of the centre-of-mass energy.

For the selection of the neutral V^0 decays (see also Ref. [14]) all combinations of tracks with opposite charge and with momenta higher than 150 MeV are examined. Both tracks must originate from a common secondary vertex with acceptable χ^2. For the final selection and for the assignment of the different hypotheses K^0, Λ and $\bar{\Lambda}$, the most important cuts are given below:

a) A χ^2 test of energy-momentum conservation for a given hypothesis, assuming that the decaying particle is produced at the primary vertex and that it decays at a secondary vertex [15].

b) Cuts on the impact parameter D of the secondary tracks from the V^0 decay with respect to the primary vertex. If D_r is the component of D in the direction perpendicular to the beam axis and D_z is the component of D in the direction of the beam axis then two cuts for each secondary V^0 track are applied: $(D_r/\sigma_r)^2 > 4$ and $(D_z/\sigma_z)^2 > 4$, where σ_r and σ_z are the uncertainties on D_r and D_z.

c) For V^0 candidates with tracks having a good dE/dx measurement, the ionisation is required to be within three standard deviations of that expected for a given hypothesis.

d) Ambiguities between K^0-Λ and K^0-$\bar{\Lambda}$ hypotheses for a V^0 decay , which survived tests a) - c), are resolved by accepting the hypothesis with the best χ^2. However, if the absolute difference in the χ^2 of the two hypotheses is less than three and if a measurement of the specific ionisation of the secondary V^0 tracks is available, a choice is made on the basis of ionisation.

This selection results in a total sample of 2566 ($\Lambda\Lambda$) pairs with 2123 pairs in the Q range from 0 to 10 GeV. The selection efficiency for the ($\Lambda\Lambda$) pairs is about 25% and their purity is $\sim$90% in the range $2 < Q < 10\,\mathrm{GeV}$ and $\sim$86% in the range $0 < Q < 2\,\mathrm{GeV}$.

4 Results

4.1 The Correlation Function $C(Q)$

The measured correlation function $C(Q)$ for the ($\Lambda\Lambda$) system is shown in Fig. 1A; $C(Q)$ is determined by dividing the differential cross section of pairs in the data by that of simulated pairs from the JETSET Monte Carlo (reference sample A). One observes a clear decrease of $C(Q)$ for values of $Q < 2$ GeV, as expected if the total spin state $S = 1$ dominates. The experimental distribution was parametrised with Eqs. 2a and 2b. The results from the fit for the parameters β and R are presented in Table 1 (reference sample A).

Another method for obtaining a reference sample is the technique of event mixing (reference sample B). Pairs of Λ's or $\bar{\Lambda}$'s for the reference sample are constructed by pairing each Λ or $\bar{\Lambda}$ with the Λ's or $\bar{\Lambda}$'s of all other events. To do this one needs some common coordinate system for the Λ's or $\bar{\Lambda}$'s produced in different events. It was chosen here to use three perpendicular axes for each event defined by the eigenvalues of the sphericity tensor. The momentum of each Λ or $\bar{\Lambda}$ in an event is calculated with respect to these axes and Q for a mixed pair is then obtained from the components of the momenta in this system.

However, this method removes not only possible FD or BE correlations, but it also affects all other correlations apart from the distribution of the particle momenta which is conserved by construction. This can be seen from Figs. 2a and 2b where the cosine of the angle $\theta_{1,2}$ between Λ or $\bar{\Lambda}$ momenta in the Z rest frame is plotted. In the unmixed events most pairs are produced back to back, whereas the distribution for the mixed sample is completely symmetric. This leads to a shift in the Q distribution for the mixed pairs towards lower values of Q. The difference between normal and mixed pairs is illustrated in Fig. 3a where the Q distribution for the pairs from Monte Carlo events is divided by that of the mixed sample. The mixed Monte Carlo sample does not reproduce the original Monte Carlo sample. To overcome this problem one usually studies the double ratio of the cross sections

$$C(Q) = \Big(\frac{P(Q)_{\mathrm{data}}}{P(Q)_{\mathrm{data,mix}}}\Big) \Big/ \Big(\frac{P(Q)_{\mathrm{MC}}}{P(Q)_{\mathrm{MC,mix}}}\Big) .$$

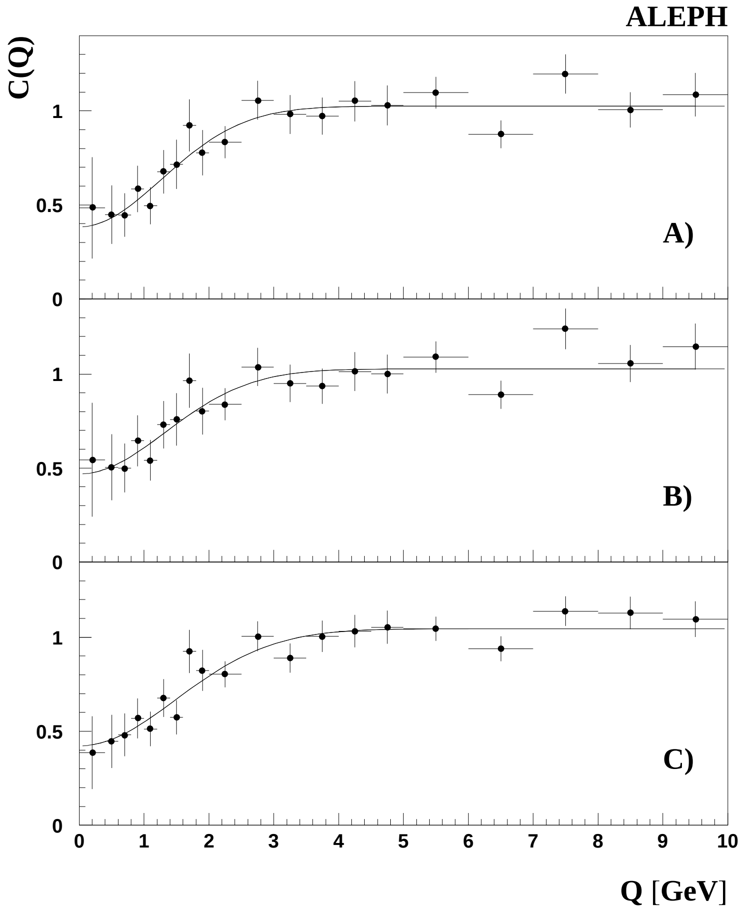

Figure 1: Correlation function $C(Q)$ for the $(\Lambda\Lambda)$ pairs using different reference samples: A) Monte Carlo, B) mixed event double ratio (see text) and C) mixed events with reweighted $\cos\theta_{1,2}$ distribution (see text). The curves represent the results of the fits using the Goldhaber parametrisation given in Eq. 2a.

The correlation function $C(Q)$ found by this procedure is displayed in Fig. 1B and is very similar to that of Fig. 1A. The fitted values for β and R (Table 1, reference sample B) agree within errors with those obtained from the distribution in Fig. 1A. This is expected because the mixed samples for data and Monte Carlo are similar, as can be seen from Fig. 3b where the ratio $P(Q)_{\mathrm{data,mix}}/P(Q)_{\mathrm{MC,mix}}$ is shown as a function of Q. It is a slowly varying function (ideally it is expected to be flat) and thus it provides only minor corrections to the correlation function as shown in Fig. 1A.

As it is found that the symmetrization of the $\cos\theta_{1,2}$ distribution is the main reason for the difference in the Q distributions of the mixed and the original pairs, a third reference sample has been constructed. For this one the data sample is mixed as described above, but the sample of the mixed pairs is then weighted such that it reproduces the $\cos\theta_{1,2}$ distribution from the original pairs obtained from the Monte Carlo. The corresponding

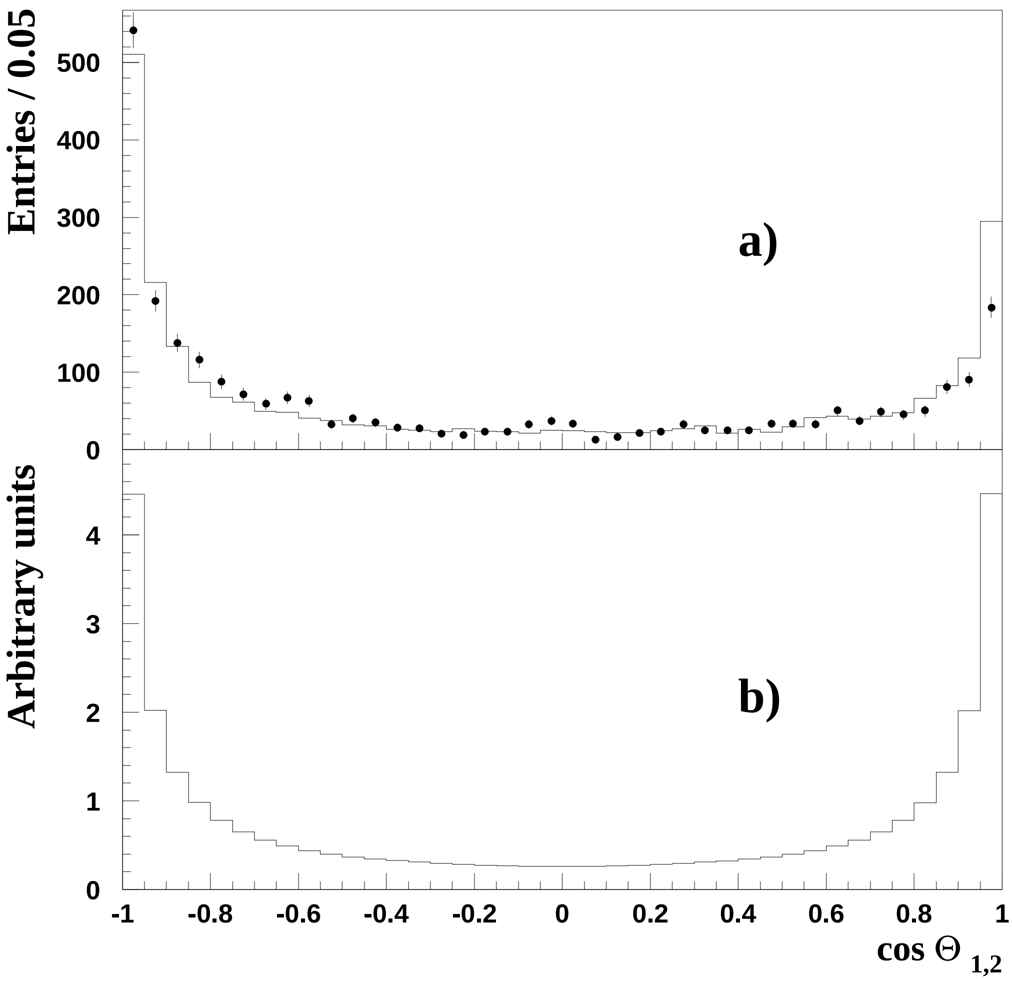

Figure 2: The histograms show the $\cos\theta_{1,2}$ distribution for a) the original ($\Lambda\Lambda$) pairs from the Monte Carlo and b) for the mixed pairs of the same sample. Points in a) show the $\cos\theta_{1,2}$ distribution of the data. The deviation of Monte Carlo from data at large $\cos\theta_{1,2}$ is due to the FD effect.

correlation $C(Q) = P(Q)_{\mathrm{data}}/P(Q)_{\mathrm{data,mix,reweighted}}$ is displayed in Fig. 1C; the smaller error bars than in the preceeding distributions reflect the larger Monte Carlo statistics used for the correction. The fitted values for β and R are in agreement with those found previously (Table 1, reference sample C). The three evaluations of $C(Q)$ based on the different reference samples are mutually consistent.

Within statistical errors the correlation function is consistent with $C(Q = 0) = 0.5$, as expected if final-state interactions (FSI) in the di-hyperon system do not contribute at threshold. FSI are expected to manifest themselves as an enhancement in the correlation function at low Q [16]. Such an effect has been measured in the $\Lambda\Lambda$ system produced in $^{12}\mathrm{C}(K^-, K^+)$ interactions at $1.66\,\mathrm{GeV}/c$ for $Q < 0.4\,\mathrm{GeV}$ [17], which corresponds to the first bin in Fig. 1. This enhancement can be attributed to FSI and/or the direct production of a di-baryon resonance with strangeness two. Even if the enhancement were only attributed

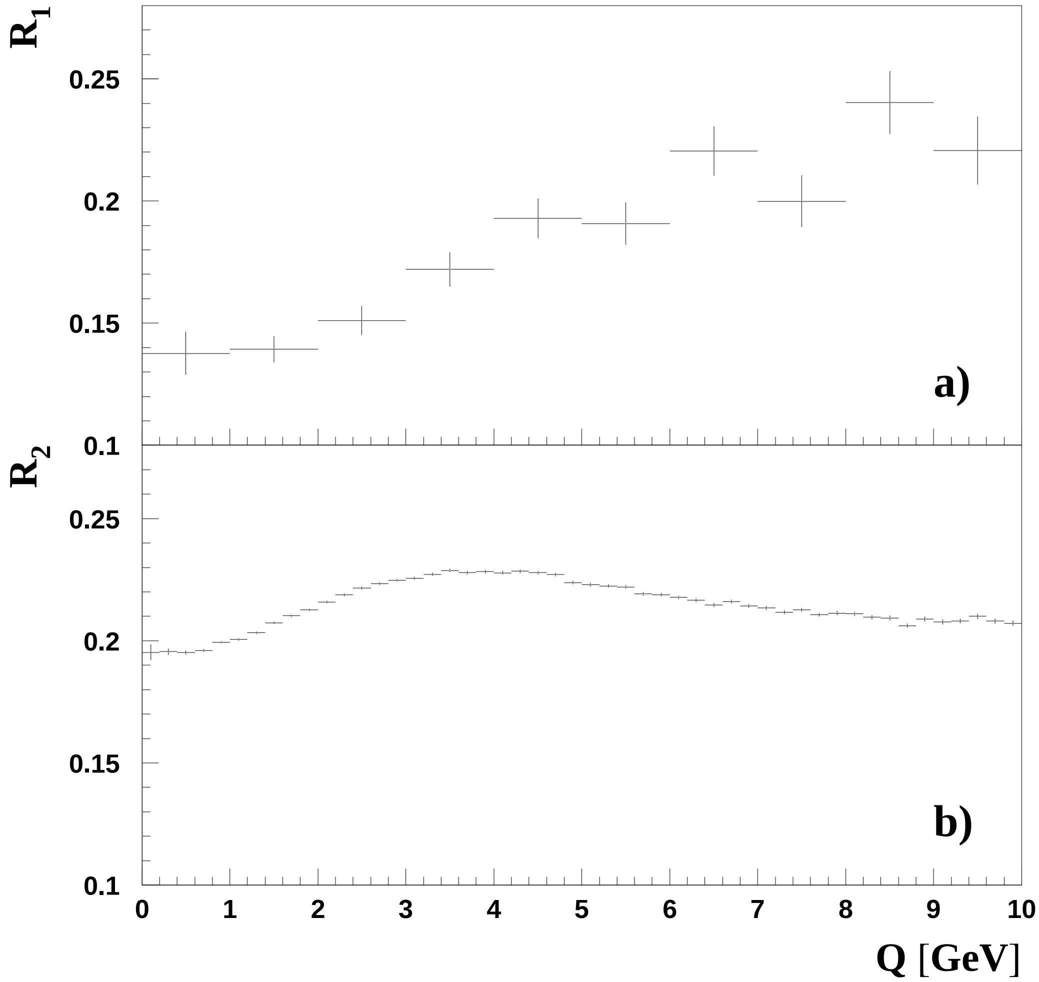

Figure 3: The ratios a) $R_1 = \frac{P(Q)_{\rm MC}}{P(Q)_{\rm MC,mix}}$ and b) $R_2 = \frac{P(Q)_{\rm data,mix}}{P(Q)_{\rm MC,mix}}$ plotted in arbitrary units. The zero is suppressed on the vertical scale.

to FSI, the magnitude of this effect is too small to be observable with the present data.

Within statistics, both Eqs. 2a and 2b result in acceptable fits and cannot be distinguished. Taking the rms variation of the central values in Table 1 for the parametrisations with Eqs. 2a and 2b as a measure of the systematic uncertainty, the resulting values for R and β are

$$\begin{aligned} R &= 0.11 \pm 0.02_{\rm stat} \pm 0.01_{\rm sys}\,\rm fm \\ \beta &= -0.59 \pm 0.09_{\rm stat} \pm 0.04_{\rm sys} \end{aligned}$$

for Eq. 2a and

$$\begin{aligned} R &= 0.12 \pm 0.04_{\rm stat} \pm 0.02_{\rm sys}\,\rm fm \\ \beta &= -0.82 \pm 0.15_{\rm stat} \pm 0.08_{\rm sys} \end{aligned}$$

for Eq. 2b. The given systematic errors account for the uncertainty in the choice of the reference sample. The difference in the results for fits with Eqs. 2a and 2b give an

Table 1: The values for β and R obtained from fits of Eqs. 2a and 2b to the correlation function $C(Q)$ for the three different reference samples A, B and C described in the text. The errors are statistical.

reference sample		β	R [fm]	χ^2/ndf
JETSET, A	Eq. 2a	-0.62 ± 0.09	0.11 ± 0.02	0.72
	Eq. 2b	-0.90 ± 0.16	0.14 ± 0.04	0.84
mixed events, B	Eq. 2a	-0.54 ± 0.10	0.11 ± 0.03	0.80
	Eq. 2b	-0.75 ± 0.16	0.13 ± 0.05	0.79
reweighted mixed events, C	Eq. 2a	-0.60 ± 0.07	0.10 ± 0.02	0.81
	Eq. 2b	-0.82 ± 0.11	0.11 ± 0.03	0.80

indication of the uncertainty due to the choice of the parametrisation for $C(Q)$. Additional contributions to the systematic errors were studied by varying the selection criteria and by removing from the fits the points below $Q < 0.6\,\mathrm{GeV}$ where background is highest. These contributions were estimated to be $\Delta R_{\mathrm{sys}} = 0.004\,\mathrm{fm}$ and $\Delta\beta_{\mathrm{sys}} = 0.024$, which are negligible compared to the errors above.

4.2 The Spin Composition $\varepsilon(Q)$

The measurement of the di-hyperon spin content $\varepsilon(Q)$ described in Section 2 has the advantage of not needing a particular reference sample. Figure 4 shows the corrected experimental angular distributions $dN/dy^*|_{\mathrm{corr}}$ for the $(\Lambda\Lambda)$ system in three intervals of Q. To account for losses due to acceptance effects and for background contributions the angular distributions have been corrected by multiplying $dN/dy^*|_{\mathrm{data}}$ by a factor obtained from Monte Carlo:

$$dN/dy^*|_{\mathrm{corr}} = dN/dy^*|_{\mathrm{data}} \frac{dN/dy^*|_{\mathrm{MC,generator}}}{dN/dy^*|_{\mathrm{MC,with\ detector\ simulation}}} .$$

The results for the relative contributions $\varepsilon(Q)$ of the spin $S = 1$ state, which are obtained by fitting Eq. 4 to the corrected distributions, are given in Table 2 and plotted in Fig. 5 together with the results for the $\Lambda\bar{\Lambda}$ system. (For the $\Lambda\bar{\Lambda}$ system Eq. 4 must be modified by replacing α_Λ^2 by $-\alpha_\Lambda^2$ [9].) The systematic errors in Table 2 were estimated by varying the analysis cuts.

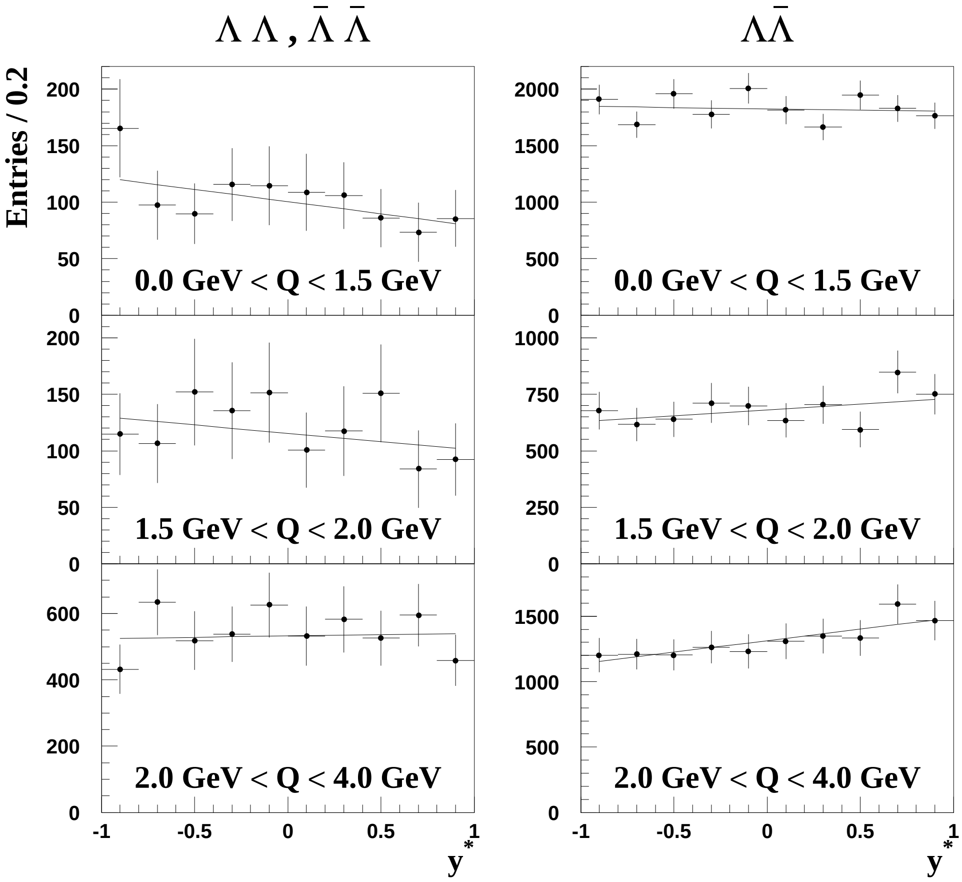

Figure 4: The corrected distributions $dN/dy^*|_{\rm corr}$ obtained for the $(\Lambda\Lambda)$ and $\Lambda\bar{\Lambda}$ data. The lines show the fits of the theoretical dN/dy^* given in Eq. 4.

For $Q > 2$ GeV the $(\Lambda\Lambda)$ system is dominated by the $S = 1$ spin state, whereas for $Q < 2$ GeV this state is suppressed compared to the $S = 0$ spin state. Such behaviour is expected from the correlation function $C(Q)$, which also decreases for values of Q below 2 GeV. For the $\Lambda\bar{\Lambda}$ system, which is free from FD correlations, the $S = 1$ spin state is consistent in the whole region of $0 < Q < 4\,\text{GeV}$.

To estimate the size R of the source, the expression of Eq. 5 was fitted to $\varepsilon(Q)$. The results of the fits are given in Table 3 without and with γ as a free parameter and displayed in Fig. 5 for γ fixed to one. To compare with other experiments $\varepsilon(Q)$ was also fitted to a Goldhaber parametrisation

$$\varepsilon(Q) = 0.75(1 - \gamma \exp(-R^2 Q^2)) \; , \tag{5a}$$

which corresponds to Eq. 5 with the denominator set to one. This approach was suggested by the OPAL Collaboration [18] and it was also used by the DELPHI Collaboration [19]. Because of the additional denominator in Eq. 5 the values of R obtained from Eq. 5 are smaller than those from Eq. 5a.

Table 2: The values of ε for the $(\Lambda\Lambda)$ and $\Lambda\bar{\Lambda}$ samples.

Q Range [GeV]	$\varepsilon(\Lambda\Lambda)$	$\varepsilon(\Lambda\bar{\Lambda})$
0.0 – 1.5	$0.36 \pm 0.30_{\text{stat}} \pm 0.08_{\text{sys}}$	$0.77 \pm 0.07_{\text{stat}} \pm 0.03_{\text{sys}}$
1.5 – 2.0	$0.52 \pm 0.31_{\text{stat}} \pm 0.10_{\text{sys}}$	$0.61 \pm 0.13_{\text{stat}} \pm 0.07_{\text{sys}}$
2.0 – 4.0	$0.78 \pm 0.16_{\text{stat}} \pm 0.09_{\text{sys}}$	$0.51 \pm 0.11_{\text{stat}} \pm 0.12_{\text{sys}}$

Table 3: The values for R obtained from fits of Eq. 5 and of Eq. 5a to $\varepsilon(Q)$ for $Q < 4\,\text{GeV}$.

Fit	γ	R [fm]
Eq. 5	1.0_{fixed}	$0.14 \pm 0.09_{\text{stat}} \pm 0.03_{\text{sys}}$
	$0.84 \pm 0.48_{\text{stat}} \pm 0.12_{\text{sys}}$	$0.11 \pm 0.09_{\text{stat}} \pm 0.03_{\text{sys}}$
Eq. 5a	1.0_{fixed}	$0.17 \pm 0.13_{\text{stat}} \pm 0.04_{\text{sys}}$

The fitted values for R from the spin composition function $\varepsilon(Q)$ and from the correlation function $C(Q)$ are in good agreement (Tables 1 and 3). They also agree within errors with those obtained from $\varepsilon(Q)$ by the OPAL and the DELPHI Collaborations. Comparing the measured radii for identical charged pions $R(\pi^\pm, \pi^\pm) = 0.65 \pm 0.04 \pm 0.16\,\text{fm}$ [20], identical charged kaons $R(K^\pm, K^\pm) = 0.48 \pm 0.04 \pm 0.07\,\text{fm}$ [21] and the $(\Lambda\Lambda)$ system $R(\Lambda\Lambda) = 0.11 \pm 0.02 \pm 0.01\,\text{fm}$ measured in hadronic Z decays indicates that the size of the source decreases with increasing mass of the emitted particles (see discussion in Ref. [22]).

5 Conclusions

The two-particle correlation function $C(Q)$ of the $(\Lambda\Lambda)$ system has been measured as a function of the Lorentz invariant variable Q. Independent of the reference sample used, $C(Q)$ shows a decrease for $Q < 2$ GeV. If this is interpreted as a FD effect, the size of the source R estimated from $C(Q)$ with a Goldhaber parametrisation (Eq. 2a) is $R = 0.11 \pm 0.02_{\text{stat}} \pm 0.01_{\text{sys}}\,\text{fm}$. This is consistent with the spin composition measurement

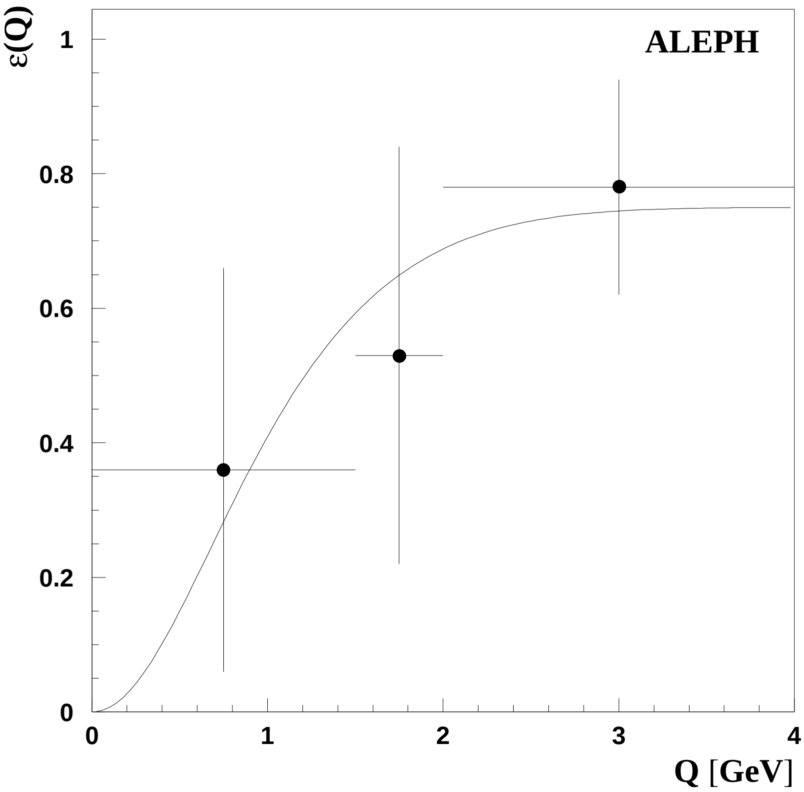

Figure 5: The fraction $\varepsilon(Q)$ of the $S = 1$ contribution for the $(\Lambda\Lambda)$ data. The curve represents the result of a fit using the parametrisation given in Eq. 5 for γ fixed to one.

of $\varepsilon(Q)$, which indicates $\varepsilon < 0.75$ for $Q < 2\,\mathrm{GeV}$ and $\varepsilon \simeq 0.75$ for $Q > 2\,\mathrm{GeV}$. The size of the source R estimated from $\varepsilon(Q)$ is $R = 0.14 \pm 0.09_{\mathrm{stat}} \pm 0.03_{\mathrm{sys}}\,\mathrm{fm}$. For the $\Lambda\bar{\Lambda}$ system, which is free of FD correlations, the spin composition measurements $\varepsilon(Q)$ are consistent with $\varepsilon = 0.75$ in the entire Q range analysed. The results for $\varepsilon(Q)$ are in agreement with the measurements of $\varepsilon(Q)$ from OPAL [18] and DELPHI [21]. Comparing the results for R with those measured in systems of identical pions and kaons indicates a decrease of R with the mass of the particles involved.

Acknowledgements

It is a pleasure to thank our colleagues in the accelerator divisions of CERN for the excellent performance of LEP. Thanks are also due to the technical personnel of the collaborating institutions for their support in constructing and maintaining the ALEPH experiment. Those of us from non-member states thank CERN for its hospitality.

References

[1] G.I. Kopylov and M.I. Podgoretskiĭ, *"Correlations of Identical Particles Emitted by Highly Excited Nuclei"*, Sov. J. Nucl. Phys. 15 (1972) 219; *"Multiple production and interference of particles emitted by moving sources"*, Sov. J. Nucl. Phys. 18 (1974) 336; G.I. Kopylov, *"Like Particle Correlations as a Tool to Study the Multiple Production Mechanism"*, Phys. Lett. B50 (1974) 472

[2] G. Cocconi, *"Second-Order Interference as a Tool for the Determination of Hadron Fireball Dimensions"*, Phys. Lett. B49 (1974) 459

[3] R. Hanbury-Brown and R.Q. Twiss, *"Correlation Between Photons in two Coherent Beams of Light"*, Nature 177 (1956) 27; *"A Test of a new Type of Stellar Interferometer on Sirius"*, Nature 178 (1956) 1046

[4] T. Sjöstrand and M. Bengtsson, *"The Lund Monte Carlo for Jet Fragmentation and e^+e^- Physics - Jetset Version 6.3 - An Update"*, Comp. Phys. Commun. 43 (1987) 367

[5] G. Goldhaber et al., *"Influence of Bose-Einstein Statistics on the Antiproton-Proton Annihilation Process"*, Phys. Rev. 120 (1960) 300

[6] T. Csörgö, *"Shape Analysis of Bose-Einstein Correlation Functions"*, Contribution to the Proceedings of the Cracow Workshop on Soft Physics and Fluctuations, Cracow, Poland (1993), World Scientific, ed R. Hwa

[7] R. Lednický and M.I. Podgoretskiĭ, *"Interference of identical particles emitted by sources of various sizes"*, Sov. J. Nucl. Phys. 30 (1979) 432

[8] B. Lörstad, *"Boson Interferometry: A Review of High Energy Data and its Interpretation"*, Int. J. Mod. Phys. A4 (1989) 2861; M.G. Bowler, *"Bose Einstein Symmetrisation, Coherence and Chaos; with Particular Application to e^+e^- Annihilation"*, Z. Phys. C29 (1985) 617

[9] G. Alexander and H.J. Lipkin, *"Use of spin-correlations to study low energy $\Lambda\Lambda$ and $\bar{\Lambda}\bar{\Lambda}$ space symmetries and resonances"*, Phys. Lett. B352 (1995) 162

[10] E. P. Wigner, *"Einige Folgerungen aus der Schrödingerschen Theorie für die Termstrukturen"*, Z. f. Phys. 43 (1927) 624; C. Eckart, *"The Application of Group Theory to the Quantum Dynamics of Monatomic Systems"*, Rev. Mod. Phys. 2 (1930) 305; R. Hagedorn, *"Selected Topics on Scattering Theory"*, Part 4, "Angular Momentum", CERN, Geneva and Max-Planck-Institut für Physik, Munich (1963) 184

[11] Particle Data Group, *"Review of Particle Physics"*, The Eur. Phys. J. C3 (1998) 1

[12] R. Lednický, *"On correlation and spin composition techniques"*, MPI–PhE–10 (1999)

[13] ALEPH Collaboration, *"ALEPH: A Detector for Annihilations at LEP"*, Nucl. Instr. and Meth. A294 (1990) 121; *"Performance of the ALEPH detector at LEP"*, Nucl. Instr. and Meth. A360 (1995) 481

[14] ALEPH Collaboration, *"Production of K^0 and Λ in hadronic Z decays"*, Z. Phys. C64 (1994) 361

[15] B. Rensch, *"Produktion der neutralen seltsamen Teilchen K^0s und Λ in hadronischen Z-Zerfällen am LEP-Speicherring"*, PhD Thesis, Universität Heidelberg, Sept. 1992

[16] R. Lednický and V.L. Lyuboshits, *"Effect of the final-state interaction on pairing correlations of particles with small relative momenta"*, Sov. J. Nucl. Phys. 35 (1982) 770; *"Final State Interaction Effects in Narrow Particle Pairs"*, Proceedings of the International Workshop on Particle Correlations and Interferometry in Nuclear Collisions (CORINNE90), Nantes, France, (1990) 42

[17] KEK-PS E224 Collaboration, *"Enhanced $\Lambda\Lambda$ production near threshold in the $^{12}C(K^-,K^+)$ reaction"*, Phys. Lett. B444 (1998) 267

[18] OPAL Collaboration, *"A first measurement of the $\Lambda\bar{\Lambda}$ and $\Lambda\Lambda$ ($\bar{\Lambda}\bar{\Lambda}$) spin compositions in hadronic Z^0 decays"*, Phys. Lett. B384 (1996) 377

[19] DELPHI Collaboration, *"Determination of the spin composition of $\Lambda\bar{\Lambda}$ and $\Lambda\Lambda$ $\bar{\Lambda}\bar{\Lambda}$ pairs in hadronic Z decays"*, Proceedings of the XXIX International Conference on High Energy Physics (ICHEP98), Vancouver (1998)

[20] ALEPH Collaboration, *"A study of Bose-Einstein correlations in e^+e^- annihilation at 91 GeV"*, Z. Phys. C54 (1992) 75

[21] DELPHI Collaboration, *"Kaon Interference in the Hadronic Decays of the Z^0"*, Phys. Lett. B379 (1996) 330

[22] G. Alexander, I. Cohen and E. Levin, *"The dependence of the emission size on the hadron mass"*, Phys. Lett. B452 (1999) 159